Swift heavy ion-induced modification and track formation in materials

D. Kanjilal

Nuclear Science Centre, Aruna Asaf Ali Marg, New Delhi 110 067, India

Swift heavy ions (SHI) lose energy in materials mainly through inelastic collisions with the atomic electrons. Along the trajectory, a trail of defects (point defects, defect clusters, structural phase transformation) known as latent track may be formed depending on the type of ion and its energy as well as the physical property of the materials. This damage is always created in the close vicinity of the trajectory of projectile. With the availability of high energy heavy ions from modern accelerators, swift heavy ion beams are proving to be of immense use in various fields, particularly for modification of materials through dense electronic excitation following the slowing down of swift heavy ions in material.

Introduction

WHEN an energetic ion penetrates any material, it loses energy mainly by two nearly independent processes: (i) elastic collisions with the nuclei known as nuclear energy loss $(dE/dx)_n$, which dominates at an energy of about 1 keV/amu; and (ii) inelastic collisions of the highly charged projectile ion with the atomic electrons of the matter known as electronic energy loss $(dE/dx)_e$ which dominates at an energy of about 1 MeV/amu or more. In the inelastic collision (cross-section $\sim 10^{-16}$ cm^2) the energy is transferred from the projectile to the atoms through excitation and ionization of the surrounding electrons. The amount of electronic loss in each collision varies from tens of eV to a few keV per Angstrom (Å). For a swift heavy ion (SHI) moving at a velocity comparable to the Bohr velocity of the electron the inelastic collision is the dominant mechanism for transfer of energy to the material for producing tracks when its value crosses a threshold value for track formation. The diameter and length of the track depend on the type and energy of the beam and the electrical and thermal conductivity of the material.

The passage of SHI in materials mainly produces electronic excitation of the atoms in the materials. SHI causes exotic effects in different classes of materials which otherwise cannot be generated by any other means. Quantitatively, it is capable of depositing electronic excitation energy of about 1 to 10 keV/Å in the materials. Such a large electronic excitation brings out various changes in materials. Atomic motions in the columnar defect regions generated by SHI has posed a fundamental question: how does the electronic excitation get transferred to the displacement of lattice atoms. There have been attempts to understand it by various models. The commonly referred models are Coulomb explosion[1] model and thermal spike[2] model. During the passage of SHI through materials, neighbouring positive target ions are produced by electronic excitation-induced ionization. These positive ions are mutually repulsive. The time to cover atomic sites is short in comparison to the response time of the conduction electrons. So during the passage of the ion a long cylinder containing charged ions is produced. This cylinder containing the charged ions explodes radially due to conversion of electrostatic energy to coherent radial atomic movements under Coulomb forces until ions are screened by conduction electrons. Due to the resulting cylindrical shock wave, ion tracks may be formed along the trajectory of the ion due to radial Coulomb explosion. The thermal spike model is the other competing process, which is also responsible for the formation of tracks. According to this model, during the passage of SHI the kinetic energy of the electrons ejected due to inelastic collision induced electronic excitation which is transmitted to the lattice by electron–phonon interaction in a way efficient enough to increase the local lattice temperature above the melting point of the material. The temperature increase is then followed by a rapid quenching (10^{13}–10^{14} K/s) that results in an amorphous linear structure when the melt solidifies. The detailed understanding of the basic process of modification of materials by SHI will help in engineering the properties of materials.

SHI is very useful for modification of the properties of films, foils and surface of bulk solids. It penetrates deep into the materials and produces a long and narrow disordered zone along its trajectory. The passage of SHI induces very rapidly developing processes which are difficult to observe during or immediately after their occurrence The information about these processes is stored in the resulting damage, such as size, shape and structure of defects. The degree of disorder can range

e-mail: dk@nsc.ernet.in

from point defects to a continuous amorphized zone along the ion path, commonly called latent track. SHI from the 15 UD Pelletron[3] at the Nuclear Science Centre (NSC) has been regularly used for producing modifications in various materials and their characterizations. In this article, some of the interesting modifications produced in various materials due to intense electronic excitation through inelastic collisions at various threshold values of energy loss are discussed.

Figure 1 shows a typical example of the variation of (dE/dx) of energetic silver (Ag) ions in $YBa_2Cu_3O_{7-y}$ (YBCO) due to elastic and inelastic collisions over a wide range of energy varying from 1 keV to 1 GeV based on Monte Carlo simulation of transport and range of ion in matter (TRIM)[4]. It is seen from this figure that the $(dE/dx)_e$ corresponding to inelastic electronic collision induced ionization and excitation, which can produce tracks, peaks at a beam energy of about 270 to 300 MeV. The $(dE/dx)_n$ due to elastic nuclear collision of the ion which mainly gives rise to point defects is maximum at about 150 keV. Its value is negligible at 270 MeV. For different SHI and materials combination, the value of $(dE/dx)_e$ and $(dE/dx)_n$ will differ and their peak positions will be at different energies. But the general characteristics of their peaks being widely separated in energy scale is always valid. In general, the $(dE/dx)_e$ peaks at tens to hundreds of keV energy of the beam and $(dE/dx)_n$ peaks at tens to hundreds of MeV depending on the type of ion (its energy, mass and atomic number) and the material (mass and atomic number) chosen. The value of (dE/dx) also varies accordingly. The typical range of penetration of the Ag beam inside the YBCO at various energies are also mentioned on the top axis of Figure 1. To avoid implantation of the ion inside the materials the thickness of the sample should be lower than the range of the beam. For modification of the material and for uniform S_e, thin film on a suitable substrate may be chosen. In case of thicker samples, foils or cleaved samples having thickness less than the range of ion over which $(dE/dx)_e$ is dominant and $(dE/dx)_n$ is negligible may be used. The range of 270 MeV Ag beam in YBCO is about 14 μm. The maximum value of $(dE/dx)_e$ is ~ 2.6 keV/Å at about 270 MeV whereas that of $(dE/dx)_n$ is about ten times lower at much lower energy of about 150 keV. Similarly for another high temperature superconducting material $Bi_2Sr_2CaCu_2O_{8+y}$ (BSCCO), the value of $(dE/dx)_e$ starts peaking at an energy of about 200 MeV of Ag.

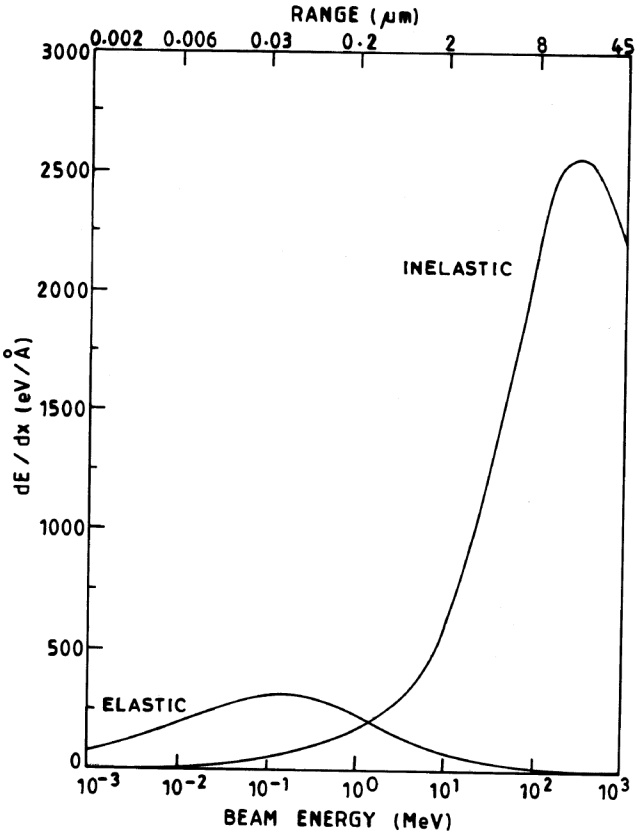

Figure 1. Variation of (dE/dx) of silver ion in $YBa_2Cu_3O_{7-y}$ due to elastic and inelastic collisions with energy in the range 1 keV to 1 GeV. Range of penetration of the Ag ion inside YBCO at various energies is given on top axis. (Reprinted from *Vacuum*, Volume number 48, pp. 979–982, copyright (1997), with permission from Elsevier Science.)

In Figure 2, the variation of $(dE/dx)_e$ and $(dE/dx)_n$ for 270 MeV Ag beam with depth as it passes through the YBCO is plotted. The energy of the SHI at different depths is also mentioned on the top axis. From this figure one can see that $(dE/dx)_e$ dominates up to a depth of about 12 μm. Near the end of range (~ 14 μm) of 270 MeV Ag beam $(dE/dx)_n$ dominates before implantation of the beam at the end of its range. So point defects and defect clusters may be formed mainly near the end of the range due to elastic collisions if the thickness of the YBCO is 14 μm or more. For a typical YBCO film of thickness 0.5 μm, the value of $(dE/dx)_e$ remains constant and the effect due to $(dE/dx)_n$ is comparatively insignificant. In fact the effect of elastic collision is comparatively negligible up to a depth of 10 μm as is evident from Figure 2.

High temperature superconductors

Controlled columnar defects produced by SHI in high temperature superconducting (HTS) materials can improve their properties for potential applications in various devices. In HTS, external magnetic field penetrates inside in the form of discrete bundles of magnetic flux lines. Each flux line has whirlpools of current called vortex. At moderate magnetic fields, movement of these vortices can impede the flow of charge carriers, leading to the destruction of superconductivity in the materials. Critical current density of HTS in magnetic field may be increased by properly controlling the movement of the vortices. Vortex lines prefer to be at the location of

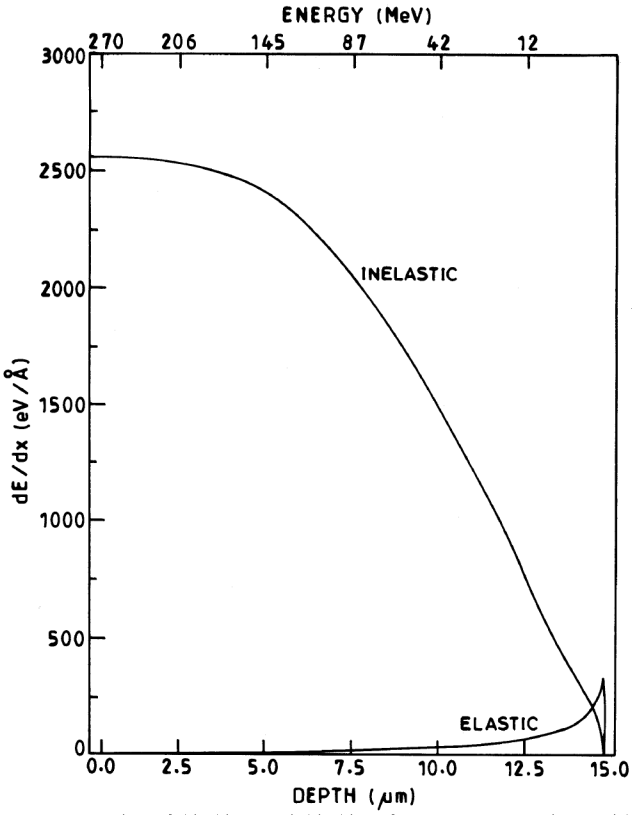

Figure 2. Plot of $(dE/dx)_e$ and $(dE/dx)_n$ for 270 MeV Ag ions with depth from the surface of $YBa_2Cu_3O_{7-y}$. The energy of the ion at different depths is mentioned on the top axis. (Reprinted from *Vacuum*, Volume number 48, pp. 979–982, copyright (1997), with permission from Elsevier Science.)

the impurity or defect sites of the material to lower their energy. Due to laminar character of the cuprates, the defects can pin the vortices in the form of pancakes rather than continuous cylinders. The enhancement of vortex pinning (or flux pinning) is of scientific and technological importance. The study of the effect of introduction of controlled columnar defects into the cuprate superconductors using swift heavy ion irradiation has been a very active area of investigation[5–14] since last decade. These defects provide a means of pinning the flux lines along its entire length rather than occasional pinning at randomly distributed point defects or impurities. Pinning force for the vortex parallel to the direction of the columns at columnar defect sites can be increased considerably if the diameter of the defect can be controlled and made close to the coherence length ξ. By precisely controlling the type and quality of the defects and its number per unit area the critical current density J_c can be improved, the irreversibility line can be shifted to higher temperature and the magnetic relaxation can be reduced. Nelson and Vinokur[15,16] predicted the existence of a Bose glass transition for vortices in a superconductor with columnar defects, for applied field less than the matching field $B_\varphi \sim \varphi\varphi_0$, where φ is the fluence (total number of ions per cm^2), φ_0 the flux quantum and B_φ the matching field at which each defect would be occupied by one vortex.

Figure 3 shows the variation microwave magneto-absorption of YBCO films with the angle of inclination measured from the film plane at various fluences ranging from 2×10^{11} cm^{-2} to 8×10^{11} cm^{-2} at 1.2 T magnetic field, 77 K temperature and 10 GHz frequency. For these studies 250 MeV silver ions from 15 UD tandem electrostatic accelerator at NSC were used for irradiation of the films. The corresponding value of $(dE/dx)_e$ is ~2.55 keV/Å. Columnar tracks were formed nearly along the c-axis of the 2000 Å YBCO c-axis oriented epitaxial film on $LaAlO_3$. Irradiation was done at an angle of 5° to avoid channeling. For microwave measurements using cavity perturbed technique, reflected power for unloaded (P_u) and loaded (P_l) cavity were measured. The magneto-absorption may be defined as

$$\Delta p = p(B, \theta, T) - p(B = 0, T),$$

where θ is inclination measured from the film plane, $p = (P_l - P_u)/P(T^+)$, $P(T^+)$ is normal state value of P.

It is clearly seen from Figure 3 that for the YBCO films irradiated along c-axis, $\Delta p(\theta)$ has a local minimum at $\theta = \theta_c$, corresponding to the angle when B is aligned with the columns. The data corresponding to different fluences are matched to the curve corresponding to the pristine sample near $\theta = 0°$. Irradiation causes a reduction in the magnitude of the magneto-absorption due to pinning of vortices at the columnar defects created by SHI.

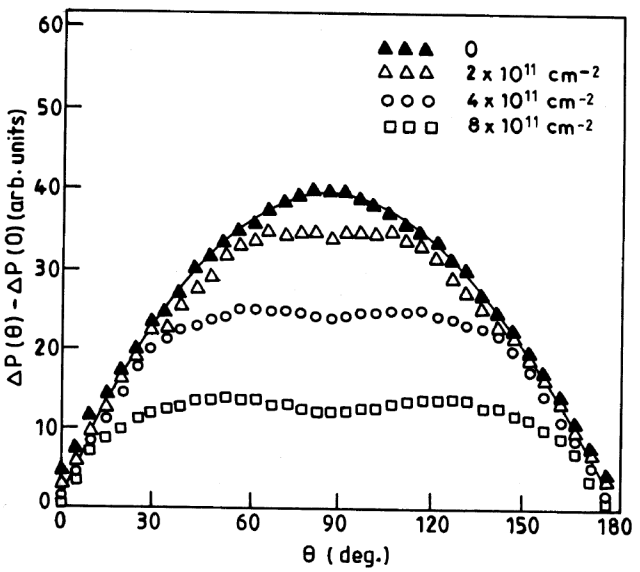

Figure 3. Variation of microwave magneto-absorption of $YBa_2Cu_3O_{7-y}$ films with the angle of inclination measured from the film plane at various fluences ranging from 2×10^{11} cm^{-2} to 8×10^{11} cm^{-2} at a magnetic field of 1.2 T at 77 K and 10 GHz frequency. (Reprinted from *Vacuum*, Volume number 48, pp. 979–982, copyright (1997), with permission from Elsevier Science.)

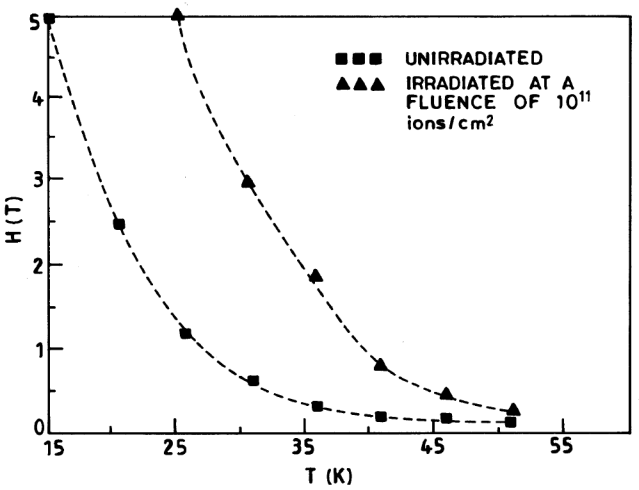

Figure 4. Shift of irreversibility lines (IL) of $Bi_2Sr_2CaCu_2O_{8+y}$ single crystal towards higher temperature due to irradiation with 200 MeV silver at a fluence of 10^{11} cm^{-2}. (Reprinted from *Vacuum*, Volume number 48, copyright (1997), pp. 979–982, with permission from Elsevier Science.)

In Figure 4, influence of SHI irradiation on the magnetically determined irreversibility lines (IL) of $Bi_2Sr_2CaCu_2O_{8+y}$ (BSSCO) cleaved single crystal is shown. The crystal was irradiated with 200 MeV silver ions corresponding to the peak value of $(dE/dx)_e$ as ~2 keV/Å. The IL shows a strong shift to higher temperature after irradiation at a fluence of 10^{11} cm^{-2}. The enhanced pinning of vortices at positions of the columnar defects caused the shift of IL to higher temperature. The columnar defects consisting of the linear amorphous channels act as highly effective vortex pinning centres.

Semiconductors

Formation of latent tracks in semiconductors using MeV ion beam[17,18] and clusters[19,20] were achieved in the last decade. The first systematic studies of track formation in evaporated films of germanium (Ge) and silicon (Si) using SHI were reported by Furno *et al.*[17] Tracks of width 23 nm in Ge film and 7 nm in Si film could be formed using 207 MeV Au^{13+} ions corresponding to the energy deposition rate of 2.6 keV/Å and 1.7 keV/Å respectively. Tracks of small crystallites or re-crystallized regions could be formed in the films due to thermal spike. From theoretical calculations of temperature distribution around the track, it was found that about half of the energy deposited through the electronic excitation by the ion contributes effectively to thermal spike resulting in the transformation. The results were interpreted in terms of time dependent line source model of thermal spike. According to this model, secondary electrons are produced with energies ranging from a few eV to a few keV in a narrow cylindrical region of ~1 nm diameter along the ion trajectory. The energy distribution of secondary electrons excited by the ion beam, various collision processes of these electrons and relaxation time in energy transfer from electrons to lattice were considered. Excited electrons with higher energy move away from the region leaving a row of positively charged ions. But the electrons with low energy are bound in this narrow region by Coulomb attraction to these positive atoms. These low energy electrons transfer their energies to the lattice by electron phonon interaction, leading to the fast (~10^{-12} s) release of thermal energy from a time dependent line source.

Formation of latent track in silicon crystal irradiated by 30 MeV fullerenes (C_{60}^{2+}) were reported in detail in 1998 by Canut *et al.*[19] and Dunlop *et al.*[20]. Large size (~10 nm diameter) continuous tracks confined around the projectile path could be observed. The tracks consisted of amorphous materials and the number of tracks corresponds to the fluence of the cluster. At this energy $(dE/dx)_e \sim 4.6$ keV/Å and $(dE/dx)_n \sim 0.0088$ keV/Å, so that $(dE/dx)_e/(dE/dx)_n \sim 50$. Due to their lower velocity ($v/c \sim 10^{-2}$) and higher mass (720 amu), fullerene projectile deposits very high energy density (10 eV/Å^3) in electronic excitation and ionization. The formation of tracks could be attributed to the strong localization of the deposited energy during the slowing down process of fullerenes in crystalline silicon. The track diameter was found to decrease much before the range of the cluster ion. The cluster breaks up into single ions or smaller assemblies of ions within a few atomic layers. The fragmented ions continue to move staying close together in a correlated manner. As the penetration depth increases, the constituents of the cluster start getting separated due to Coulomb repulsion between the charged fragments and multiple scattering in elastic collision processes. At large penetration depths (≥ 100 nm), the correlated slowing down of the cluster constituents is partially lost and deposited energy density falls rapidly and eventually drops below the threshold value for track generation. The tracks often end as a series of aligned droplets of damaged structure.

Hare *et al.*[18] demonstrated formation of amorphous tracks and amorphous layers in single-crystalline InP after swift heavy ion irradiation with 250 MeV Xe in the depth region between 35 nm and about 10 μm where electronic energy loss process is the dominant mechanism for slowing down of the ion. It was inferred that electronic energy loss per ion per unit length has to exceed a critical value of 13 keV/nm to damage single crystalline InP. The concentration and structure of the damage produced by electronic excitations depend on the ion fluence. At small fluences, only point defects and point defect complexes are formed. With increase in ion fluence discontinuous tracks and subsequently amorphous layers are formed. The fluence dependence indicates that a single ion impinging on virgin crystal-

line InP generates point defects and point-defect complexes. Amorphous track appears when a critical concentration of these defect centres is created. At higher irradiation fluence the crystallization speed of the defect region becomes smaller than the cooling rate and a continuous amorphous track is frozen in. The roughness of *c*-Si (111) surface irradiated by 200 MeV Ag^{14+} ion at an incidence angle of 15 degrees with respect to surface normal at 80 K is investigated by atomic force microscopy. The increase in roughness during irradiation is a consequence of the unsaturated dangling bonds created due to SHI-induced hydrogen desorption and spatial correlation of damage created by the individual ions beyond a critical fluence. A new type of ditch and dike structure was formed on the surface during irradiation at a fluence of 5×10^{13} ions/cm^2. This is attributed[21] to the cumulative effect of overlapping of irradiation-induced damaged zones in addition to electronic excitation-induced shear motion of atoms towards the surface.

Metallic system

It is difficult to produce latent tracks in metallic target as the large number of mobile conduction electrons present in the target screen the space charge created following the ionization of the target atoms located in the vicinity of the trajectory of projectile ion and spread the deposited energy by the ion rapidly. However, formation of tracks was reported in metallic targets such as Ni_3B (ref. 22), $NiZr_2$ (ref. 23), NiTi (ref. 24) etc. by GeV heavy ions. The tracks consist of amorphous matter located around the path of the projectile ion. They could be created only when the amount of electronic energy loss was higher than the corresponding threshold value of a few keV/Å. The configuration of the tracks gradually changes from separated droplets to continuously damaged cylinders as the value of $(dE/dx)_e$ increases above the threshold value. In pure metallic samples like titanium[25,26], tracks could be produced using GeV heavy ions ($S_e \sim 4$ keV/Å). In the vicinity of tracks, highly defective crystalline zones could be observed due to intense electronic excitation. Discontinuous damage located within an average diameter of 5 nm was observed after irradiation with GeV Pb and U beams. Ti and Zr samples, pre-thinned for electron microscopy, were irradiated with cluster ion fullerene[27,28] at 300 K to investigate track formation. Quasicontinuous tracks of diameter of about 20 nm around the projectile path were created in Ti samples. In case of Zr samples, where GeV heavy ion could not produce any damage visible by electron microscope, a fullerene beam produced strongly damaged cylindrical zones. Although the rate of energy loss $(dE/dx)_e$ may be similar for very heavy (Pb, U, etc.) mono-atomic beams at GeV and a fullerene beam at tens of MeV, the comparatively stronger spatial localization of the deposited energy during slowing down of fullerene ions causes much larger extension of damaged zones in the target.

Colossal magnetoresistance material

The influence of 250 MeV Ag ion irradiation on electrical transport and low frequency conduction noise of 3000 Å thin films of colossal magnetoresistance (CMR) material $La_{0.75}Ca_{0.25}MnO_3$ (LCMO) has been investigated[29,30]. The threshold value of S_e for columnar amorphization was estimated[2] as 1.2 keV/Å. At 250 MeV, the value of S_e is 2.4 keV/Å. So, columnar amorphization was generated throughout the thickness of the film by irradiation. Variation of metal–insulator transition temperature T_p and resistivity as a function of ion fluence was analysed. At a fluence of 10^{11} ions per cm^2 the value of T_p increased by about 10 K. Resistivity decreased in the ferromagnetic metallic state from that of the pristine sample. Further increase in fluence caused decrease in the value of T_p and corresponding increase in resistivity. At a fluence of 10^{13} ions per cm^2 the metal–insulator transition disappeared and the system became highly resistive, exhibiting semiconducting behaviour down to 77 K. The $1/f$ conduction noise of LCMO thin film showed monotonic increase with fluence. The observed behaviour of the normalized conduction noise was consistent with the general expectation of defect formation due to ionization caused during irradiation by Ag ion at an energy of 250 MeV.

Polymer

Swift heavy ions produce cylindrical damaged zones along their trajectory in polymers. This zone can be etched by suitable chemicals to produce a through hole (pore) of diameter varying from a few tens of nm to a few μm depending on etch time and etching condition for various applications. Determination of the dimension of ion damaged zone is of interest for understanding the interaction process of swift heavy ions with polymers and its application. Various techniques for probing surface morphology have been utilized[31] to measure track diameters. At NSC novel approaches were used like online Elastic Recoil Detection Analysis (ERDA) of hydrogen concentration[32] to estimate track diameter and online recording of partial pressures of evolved gases[33] to get an insight to the varying damaged zones. Electronic excitation of the constituent atoms of the polymer causes breaking of bonds associated with hydrogen (H). Free H atoms combine with each other to form hydrogen molecule. These molecules being light have high diffusivity and escape from the polymer causing reduction in H content. Each ion causes release of H from a cylindrical effective zone around its trajectory.

The decrease in H content was measured[32] online by ERDA by detecting the H recoil by a surface barrier detector. The initial slope in the plot of concentration of H as a function of ion fluence gave the cross section (πr^2, r is the track radius) of H release. At higher fluence when the track diameters start overlapping, the rate of loss of hydrogen decreased and the hydrogen loss curve started to flatten. This particular fluence can also be used to estimate the track radius. Polyethylene terephthalate (PET) was irradiated by 180 MeV Ag ions and the partial pressures of the evolved gases were monitored by a quadrupole mass analyser to determine varied damage zones[33]. The dominant components of the evolved gases were hydrogen, carbon monoxide and ethylene due to breaking bonds of PET. The logarithmic decrease in the release of gaseous products provides an estimate of track diameter. Different cross sections of release of different gases indicate that effective ion beam damage zone varies with the type of gases evolved.

Highly oriented pyrolytic graphite

In situ high vacuum scanning tunneling microscopic and scanning tunneling spectroscopic investigations on pristine and irradiated surfaces of highly oriented pyrolytic graphite (HOPG) were carried out[34] at NSC using home-built ultra high vacuum STM in the materials science beam line. The 17 Å × 17 Å STM images of pristine and 250 MeV Au ion irradiated (fluence = 2×10^{13} ions/cm^2) surfaces are shown in Figure 5. The effect of electronic excitation ($S_e \sim 2.1$ keV/Å) on the HOPG surface is clearly visible from the change in surface morphology shown in Figure 5 *b*. The STM image of the pristine sample shown in Figure 5 *a* shows a three-to-hexagonal moiré pattern where the localization of electronic wave function corresponding to the covalent bonded HOPG is clearly visible. After irradiation, the moiré pattern is smoothened out and delocalization of the electronic states is observed as shown in Figure 5 *b*. Spectroscopic studies[34] showed a nonlinear nature of *I–V* curve for pristine HOPG surface. After irradiation, the *I–V* curve for the surface showed linear variation of tunneling current with bias voltage. The ohmic behaviour of *I–V* curve along with the delocalization of covalent bonded electronic wave function suggests the development of metallic nature of HOPG surface by intense electronic excitation during SHI irradiation.

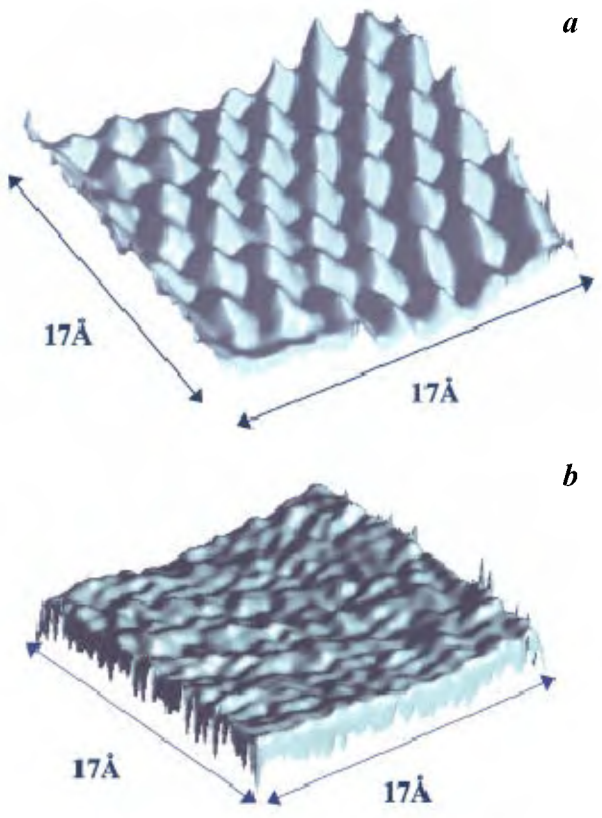

Figure 5. STM images (17 Å × 17 Å) of (***a***) pristine highly oriented pyrolytic graphite (HOPG) and (***b***) HOPG irradiated with 200 MeV Au^{+13} ions at a fluence of 2×10^{13} ions/cm^2. (Reprinted from *Vacuum*, Volume number 57, pp 319–325, Copyright (2000), with permission from Elsevier Science.)

Conclusion

The modification of properties of materials due to electronic excitation during swift heavy ion irradiation and formation of latent tracks in materials using suitable combination of projectile and target has emerged as an exciting field of research and development. The interaction of swift heavy ion with atoms of the materials is discussed. Results of electronic excitation-induced changes in the physical and chemical properties of a few systems, with emphasis on the results of some of the research work carried out at NSC, are presented in this article.

1. Leuser, D. and Dunlop, A., *Radiat. Effects Defects Solids*, 1993, **126**, 163.
2. Szenes, G., *Phys. Rev. B*, 1995, **51**, 8026.
3. Kanjilal, D., Chopra, S., Narayanan, M. M., Iyer, I. S., Jha, V., Joshi, R., and Datta, S. K., *Nucl. Instrum. Methods Phys. Res. A*, 1993, **238**, 97.
4. Ziegler, J. F., Biersack, J. P. and Littmark, U., *Stopping and Ranges of Ions in Matter*, Pergamon, New York, 1985.
5. Civale, L., Marvick, A. D., Worthington, T. K., Kirk, M. A., Thompson, J. R., Krusin-Elbaum, L., Sun, Y., Clen, J. R. and Holzberg, F., *Phys. Rev. Lett.*, 1991, **67**, 648.
6. Budhani, R. C., Holstein, W. L. and Suenega, M., *Phys. Rev. Lett.*, 1994, **72**, 566.
7. Lofland, S. E., Bhagat, S. M., Rajeswari, M., Venkatesan, T., Kanjilal, D., Senapati, L. and Mehta, G. K., *Phys. Rev. B*, 1995, **51**, 8489.
8. Pradhan, A. K., Roy, S. B., Chaddah, P., Kanjilal, D., Chen, C. and Wanklyn. B. M., *Phys. Rev.*, 1996, **B53**, 2269.

9. Lofland, S. E., Tyagi, S. D., Bhagat, S. M., Rajeswari, M., Venkatesan, T., Kanjilal, D., Senapati, L. and Mehta, G. K., *Physica C,* 1996, **267**, 79.
10. Kanjilal, D., *Vacuum*, 1997, **48**, 979.
11. Pradhan, A. K., Chen, B., Pinodoria, G., Nakao, K., Koshizuka, N., Kanjilal, D., Chowdhury, A. J. S. and Wanklyn, B. M., *Phys. Rev. B*, 1997, **55**, 11129.
12. Kumar, R., Samanta, S. B., Arora, S. K., Gupta, A., Kanjilal, D., Pinto, R. and Narlikar, A. V., *Solid State Commun.*, 1998, **106**, 805.
13. Lidmar, J. and Wallin, M., *Europhys. Lett.*, 1999, **47**, 494.
14. Kwok, W. K., Olsson, R. J., Karapetrov, G., Paulius, L. M., Moulton, W. G., Hofman, D. J. and Crabtree, G. W., *Phys. Rev. Lett.*, 2000, **84**, 3706.
15. Nelson, D. R. and Vinokur, V. M., *Phys. Rev. Lett.*, 1992, **68**, 2398.
16. Nelson, D. R. and Vinokur, V. M., *Phys. Rev. B*, 1993, **48**, 13060.
17. Furno, S., Otsu, Hojou, K. and Izui, K., *Nucl. Instrum. Methods Phys. Res. B*, 1996, **107**, 223.
18. Hare, O., Wesch, W., Wendler, E., Gaiduk, P. I., Komarov, F. F., Klaumunzer, S. and Meier, P., *Phys. Rev. B*, 1998, **58**, 4832.
19. Canut, B., Bonardi, N., Ramos, S. M. M. and Della-Negra, S., *Nucl. Instrum. Methods Phys. Res. B*, 1998, **146**, 296.
20. Dunlop, A., Jaskierowicz, G. and Della-Negra, S., *Nucl. Instrum. Methods Phys. Res. B*, 1998, **146**, 302.
21. Singh J. P., Singh, R., Kanjilal, R., Mishra, N. C. and Ganesan, V., *J. Appl. Phys.*, 2000, **87**, 2742.
22. Audouard, A., Balanzat, E., Bouffard, Jousset, J. C., Chamberod, A., Dunlop, A., Lesueur, D., Fuchs, G., Spohr, R. and Vetter, J., *Phys. Rev. Lett.*, 1990, **65**, 875.
23. Barbu, A., Dunlop, A., Lesueur, D. and Averback, R. S., *Europhys. Lett.*, 1991, **15**, 37.
24. Dunlop, A., Lesueur, D. and Barbu, *J. Nucl. Mater.*, 1993, **205**, 426.
25. Henry, J., Barbu, A., Leridon, B., Lesuer, D. and Dunlop, A., *Nucl. Instrum. Methods Phys. Res. B*, 1992, **67**, 390.
26. Dammak, H., Barbu, A., Dunlop, A., Lesueur, D. and Lorenzelli, *Philos. Mag. Lett.*, 1993, **67**, 253.
27. Dammak, H., Dunlop, A., Lesueur, D., Brunelle, A., Della-Negra, S. and Le Beyec, Y., *Phys. Rev. Lett.*, 1995, **74**, 1135.
28. Dunlop, A., Dammak, H. and Lesueur, D., *Nucl. Instrum. Methods Phys. Res. B*, 1996, **112**, 23.
29. Arora, S. K., Kumar, R., Singh, S., Kanjilal, D. and Mehta, G., K., *J. Appl. Phys.*, 1999, **86**, 4452.
30. Kumar, R., Arora, S. K., Kanjilal, D., Mehta, G. K., Bathe, R., Date, S. K., Shinde, S. R., Saraf, L. V., Ogale, S. B. and Patil, S. I., *Radiat. Effects Defects Solids*, 1999, **147**, 187.
31. Trautman, C., *Nucl. Instrum. Methods Phys. Res. B*, 1995, **105**, 81.
32. Mittal, V. K., Lotha, S. and Avasthi, D. K., *Radiat. Effects Defects Solids*, 1999, **147**, 199.
33. Avasthi, D. K., Singh, J. P., Biswas, A. and Bose, S. K., *Nucl. Instrum. Methods Phys. Res. B*, 1998, **146**, 504.
34. Singh, J. P., Tripathi, A. and Kanjilal, D., *Vacuum*, 2000, **57**, 319.

ACKNOWLEDGEMENTS. I thank members of Materials Science group and Pelletron group for their contributions to various experiments performed at NSC. Generous financial support received from DST in the form of IRPHA project for setting up Materials Science beam line with experimental facilities, and in the form of a research project for fabrication of *in situ* UHV STM are gratefully acknowledged.